11-1-2010

MAS Pole Location and Effective Spatial Bandwidth of the Scattered Field

James Richie
Marquette University, james.richie@marquette.edu

Published version. *IEEE Transactions on Antennas and Propagation* (November 2010), DOI: 10.1109/TAP.2010.2071346.

MAS Pole Location and Effective Spatial Bandwidth of the Scattered Field

James E. Richie, *Senior Member, IEEE*

***Abstract*—The concept of effective spatial bandwidth (EBW) is introduced for periodic domains. The EBW is applied to the incident and scattered fields along the boundary of an infinite circular cylinder. The scattered field is formulated using the method of auxiliary sources (MAS). In MAS, monopoles on an auxiliary surface (AS) are used to model the scattered field. It is shown that the EBW of the incident field can provide some insight regarding the placement of poles for the MAS scattered field model. Example simulations are provided to demonstrate the usefulness of EBW with respect to monopole placement rules in MAS.**

***Index Terms*—Boundary value problems, electromagnetic scattering.**

I. Introduction

THE generalized multipole technique (GMT) [1] and its variations can be used to compute the scattering from objects in a variety of scenarios. GMT and related methods compute the scattering from perfectly conducting objects by placing canonical sources within the object to model the scattered field. Often, discrete multipoles are used for this purpose.

One variation within the family of GMT methods is the method of auxiliary surfaces (MAS) [2]. In MAS, an auxiliary surface (AS) is defined within the scatterer. The canonical sources are placed on the AS. Typically, monopoles are used for two-dimensional scattering problems and Hertzian dipoles are used for three-dimensional scatterers. Recently, a three-dimensional quasistatic MAS formulation has been reported in [3].

The major questions that arise when implementing GMT methods pertain to the location and number of poles necessary to obtain a sufficiently accurate solution. One approach to determining the location and number of poles is to develop rules based on qualitative information and experience. In [4] an empirical scheme is proposed to determine the location and number of monopole origins for two-dimensional scattering problems. In [5], a rule-based algorithm is used to determine appropriate multipole origins for GMT. Pole location, number and placement issues are also discussed in [6], and [7].

Monopole location in MAS is governed by the AS. Desirable characteristics for the AS are reviewed in [2]. In particular, the auxiliary surface must enclose the singularities of the scattered field. Studies of this requirement appear in [1, Ch. 5] and [8].

Manuscript received July 15, 2009; revised April 13, 2010; accepted April 14, 2010. Date of publication August 30, 2010; date of current version November 03, 2010.

The author is with the Department of Electrical and Computer Engineering, Marquette University, Milwaukee, WI 53233 USA (e-mail: james.richie@mu.edu).

Digital Object Identifier 10.1109/TAP.2010.2071346

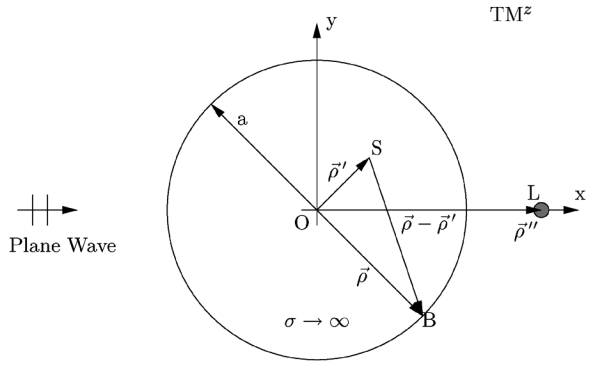

Fig. 1. Geometry of the two-dimensional scattering problem.

A second approach to determining the location and number of poles is to study the convergence and accuracy of the numerical method. It is possible to infer useful guidelines from the results of such studies. Investigations concerning the convergence and accuracy of MAS for the perfectly conducting circular cylindrical scatterer (as shown in Fig. 1) have been reported in [9] and [10].

In [9], a monopole line source in the vicinity of the cylinder is investigated. For a cylinder of radius a and a monopole line source at $\vec{\rho}''$ (point L in Fig. 1), the singularity in the scattered field is at a radius of a^2/ρ''. Therefore, the AS radius must be chosen between a^2/ρ'' and a. In [9], AS radius choices both inside and outside this requirement are investigated.

In [10], the numerical accuracy and analytical accuracy of MAS are described in detail. It is shown that the numerical accuracy dominates the error when the AS radius is very small. To understand the significance of a small AS radius, consider the geometry of Fig. 1. The addition theorem is used to write the field at $\vec{\rho}$ due to a unit strength monopole at $\vec{\rho}'$ as an expansion of multipoles at the origin (with $\rho' < \rho$) [11]

$$H_o^{(2)}\left(k|\vec{\rho} - \vec{\rho}'|\right) = \sum_{n=-\infty}^{\infty} J_n(k\rho')H_n^{(2)}(k\rho)e^{jn(\phi-\phi')} \quad (1)$$

where k is the wavenumber $(2\pi/\lambda)$, $J_n(\cdot)$ is the Bessel function of the first kind of order n, and $H_n^{(2)}(\cdot)$ is the Hankel function of the second kind of order n representing outward traveling waves. Eqn. (1) demonstrates that a monopole at $\vec{\rho}'$ is equivalent to a multipole expansion at the origin. When the AS radius (ρ') is zero (an extreme case), only the $n = 0$ term of the expansion is non-zero. When ρ' is small, the multipole expansion has small coefficients except near $n = 0$. Thus, there is only a small amount of variation in the monopole field along the boundary $\rho = a$ if the AS radius is small.

However, as $\rho' \to a$, the left hand side of (1) indicates that the field becomes nearly singular at $\phi = \phi'$. In other words, the amount of variation in the field along $\rho = a$ becomes very large as the AS radius approaches the cylinder radius.

In this paper, the following question is investigated. For the geometry of Fig. 1, how much variation in the field along the boundary due to the MAS monopoles is necessary to obtain a suitable solution? Certainly a small AS radius admits small variation and an AS radius near a admits large variation of the fields along the boundary. It is the incident field variation along the boundary that determines how much variation is needed from the MAS monopole field.

It is believed that a fundamental understanding of the relationship between the amount of incident field variation and monopole placement can be used in a wide variety of situations and lead to additional guidelines for monopole placement in general problems.

The intent of this work is to use a well-known problem to obtain some physical insight into the effect of monopole placement in the MAS method. The work presented here is not intended to introduce a new, more efficient implementation of MAS; rather, the results obtained by this investigation provide valuable physical insight to the more general problem.

The analysis presented here includes a procedure to quantify the amount of variation of fields along the boundary. The result will be denoted as the effective spatial bandwidth (or EBW) of the field. Next, the EBW for the incident field along the boundary will be computed both analytically and numerically. The scattered field EBW will also be presented, both for the analytic solution to the circular scatterer, and for the MAS monopole. Example simulations will then be described and discussed. The examples shall demonstrate the effectiveness of EBW as an engineering tool to aid in the placement of monopoles in the MAS technique.

II. Boundary Field Bandwidth

The concept of spatial bandwidth of fields for non-periodic domains is discussed in [12]. Bandwidth can be thought of as a measure of the frequency content or amount of variation of a signal or function. In this paper, the terms "bandwidth" and "frequency" refer to the degree of spatial variation of field quantities.

In many cases, the absolute bandwidth is infinite because there is non-zero energy over the entire spectrum. The energy asymptotically approaches zero as the frequency becomes large enough. This asymptotic behavior is typical for scattered fields [12]. Thus, it is convenient to define the bandwidth as the range of frequencies that contain a (usually large) percentage of the total energy of the function.

The bandwidth of a function $f(x)$ can be computed either in the spectral domain or in the original domain using convolution. In the spectral domain, the spatial frequency content is computed and the bandwidth can be estimated from the spectrum.

Consider estimating the bandwidth via convolution. One approach is as follows. First, the function is bandlimited. Consider $f(x)$ with domain $-\infty < x < \infty$. The convolution

$$f_w(x) = \frac{1}{\pi} \int_{-\infty}^{\infty} \frac{\sin\left[w(x-\xi)\right]}{(x-\xi)} f(\xi) d\xi \tag{2}$$

results in the band-limited function $f_w(x)$ with maximum frequency w. For frequencies below w, the spectral content of $f(x)$ and $f_w(x)$ are identical. To estimate the bandwidth, the function $f_w(x)$ is computed for increasing w until the difference in energy between $f_w(x)$ and $f(x)$ becomes smaller than some pre-defined threshold.

In the present problem, the function is a field quantity on the boundary of a scatterer. The field quantity has a spatial or effective bandwidth (EBW) that quantifies the amount of variation (or spatial frequency content) of the field quantity.

Consider the scattering of an incident field by a conducting circular cylinder as shown in Fig. 1. The cylinder is uniform and of infinite extent in z. The incident fields considered will be TM^z. The uniformity in z allows the scattering problem to be solved in the $x - y$ plane.

A field quantity $e(\phi)$ (e.g., an incident or scattered field component) will be a periodic function of ϕ around the surface of the scatterer. Because the period of ϕ is 2π, the fundamental spatial frequency is one and the harmonics are integers. The bandlimited function $e_N(\phi)$ limited to a maximum spatial frequency of N (an integer) can be determined using

$$e_N(\phi) = \frac{1}{C} \int_0^{2\pi} B_N(\phi, \xi) e(\xi) \rho(\xi) d\xi \tag{3}$$

where C is the circumference of the scatterer, $\rho(\phi)$ is the distance from the origin to the point on the scatterer at angle ϕ, and

$$B_N(\phi, \xi) = \frac{\sin\left[\left(N + \frac{1}{2}\right)(\phi - \xi)\right]}{\sin\left[\frac{1}{2}(\phi - \xi)\right]}. \tag{4}$$

Note that the $N = 0$ term represents the average value of $e(\phi)$. The functions $\exp\{\pm jn\phi\}$, or equivalently $\sin n\phi$ and $\cos n\phi$ with integer n, represent the spatial harmonic functions for periodic domain ϕ considered in this work.

The effective spatial bandwidth of the field shall be denoted as EBW. For a periodic function $e(\phi)$, define $EBW = N$ such that N is the smallest integer with $\Delta_N \leq 0.01\%$ where

$$\Delta_N = \frac{\mathcal{E}(e) - \mathcal{E}(e_N)}{\mathcal{E}(e)} \times 100\% \tag{5}$$

and

$$\mathcal{E}(e) = \int_0^{2\pi} |e(\phi)|^2 \rho(\phi) d\phi \tag{6}$$

where e_N is the bandlimited form of e, as given by (3) and (4).

A. Incident Field Effective Bandwidth

In this section, the effective bandwidth of the incident field is computed. Both the case of a plane wave incident field and a monopole line source are considered. In each case, the incident field is normalized to unit strength, i.e., $E_o = 1$.

1) Plane Wave Incident Field: Consider a plane wave incident on the cylinder, traveling in the $+x$ direction, as shown in Fig. 1. The electric field is given by $\vec{E} = E_z^p \hat{e}_z$ where

$$E_z^p = e^{-jkx} = e^{-jk\rho\cos\phi} = \sum_{n=-\infty}^{\infty} j^{-n} J_n(k\rho) e^{jn\phi} \tag{7}$$

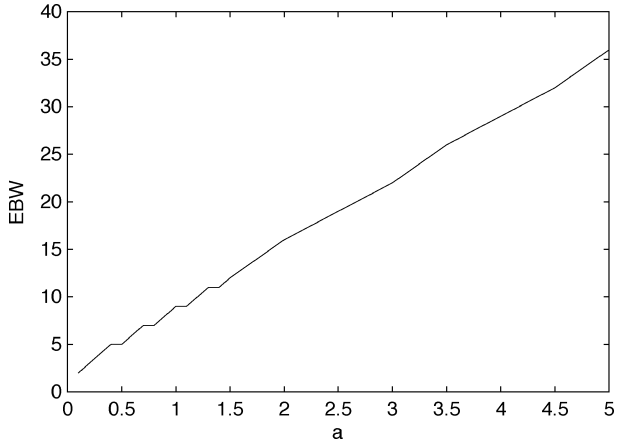

Fig. 2. EBW for a plane wave incident on a cylinder of radius $a(\lambda)$.

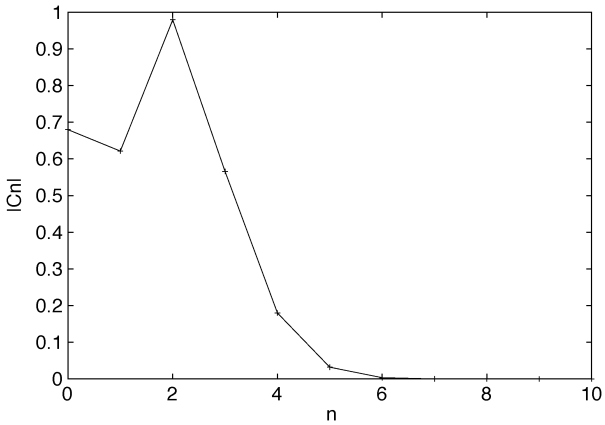

Fig. 3. $|c_n|$ for case a $= 0.5\lambda$; EBW for incident field is $N = 5$.

where the superscript p indicates that the incident field is a plane wave.

The effective bandwidth of E_z^p on the surface of a cylinder of radius a can be investigated using (3). After some manipulation

$$E_{z,N}^p(\phi) = \frac{1}{2\pi} \sum_{n=-\infty}^{\infty} \left[j^{-n} J_n(ka)\right] \int_{\xi=0}^{2\pi} B_N(\phi,\xi) e^{jn\xi} d\xi \quad (8)$$

where $E_{z,N}^p$ is the bandlimited form (with maximum frequency N) of E_z^p.

Consider (8). Since all values of n are allowed in the sum, the absolute bandwidth of E_z^p is infinite. However, the coefficient of each term is proportional to the quantity in brackets in (8). The quantity in brackets converges to zero as $|n| \to \infty$.

For the case of a circular cross section, (8) also demonstrates that the wave transformation in (7) results in the spectral content of the field around the circular boundary. Note that this is only true for the circular case.

The effective bandwidth for the plane wave can also be computed by numerically integrating (3) and (6). A graph showing the EBW vs. cylinder radius (in wavelengths) is shown in Fig. 2. As the radius increases, the EBW for a plane wave around the circumference of the cylinder increases, as expected.

2) Monopole Line Source Incident Field: Consider a monopole line source at $(\rho'', 0)$, labeled L in Fig. 1. The incident field is $E_z^o = H_o^{(2)}(k|\vec{\rho} - \vec{\rho}''|)$. The field E_z^o along the cylinder boundary can be written using the addition theorem [11]

$$E_z^o = \sum_{n=0}^{\infty} \varepsilon_n H_n^{(2)}(k\rho'') J_n(ka) \cos n\phi \quad (9)$$

where the superscript o indicates a monopole line source, and ε_n is 1 if $n = 0$ and 2 otherwise.

The bandlimited form of E_z^o can be computed

$$E_{z,N}^o = \frac{1}{2\pi} \sum_{n=0}^{\infty} \left[\varepsilon_n H_n^{(2)}(k\rho'') J_n(ka)\right] \times \int_{\xi=0}^{2\pi} B_N(\phi,\xi) \cos n\xi \, d\xi. \quad (10)$$

Again, the expression for $E_{z,N}^o$ indicates that the absolute bandwidth is infinite. The effective bandwidth depends on the behavior of the term in brackets. Calculation of EBW indicates that the EBW is large for small ρ''/a and approaches the plane wave bandwidth as ρ''/a becomes large, as expected.

B. Scattered Field Bandwidth

In this section the effective bandwith of the scattered field along the boundary is considered. The analytic solution model and the MAS model for the scattered field are discussed.

1) Analytic Solution Case: First, consider the analytic solution to the circular cylindrical problem shown in Fig. 1

$$E_z^a = \sum_{n=-\infty}^{\infty} c_n H_n^{(2)}(k\rho) e^{jn\phi} \quad (11)$$

where the superscript a indicates the analytic solution. For a plane wave incident field (8), the coefficients are given by

$$c_n = -j^{-n} \frac{J_n(ka)}{H_n^{(2)}(ka)}. \quad (12)$$

Equation (11) represents the scattered field as a multipole expansion where all poles are at the origin. The bandlimited function corresponding to E_z^a can be found using (3)

$$E_{z,N}^a = \frac{1}{2\pi} \sum_{n=-\infty}^{\infty} H_n^{(2)}(ka)[c_n] \int_{\xi=0}^{2\pi} B_N(\phi,\xi) e^{jn\xi} \, d\xi. \quad (13)$$

Once again, the absolute bandwidth is infinite and the effective bandwidth depends on the coefficients in (13). In this case, however, $|H_n^{(2)}(ka)| \to \infty$ as n increases. As seen in (12), c_n approaches 0 at a faster rate.

Each term of the sum in (13) can also be considered to have an EBW. Since (11) is a spectral expansion of the scattered field along the boundary, the EBW for the n^{th} term is n.

It is illuminating to compare the coefficients c_n with the effective bandwidth of the incident field for a particular problem. Fig. 3 shows $|c_n|$ vs. n for the case of a 0.5λ radius cylinder. Note that the incident field, a plane wave, has an EBW of $N = 5$. The fifth term in the series $(n = \pm 5)$ has an EBW that matches

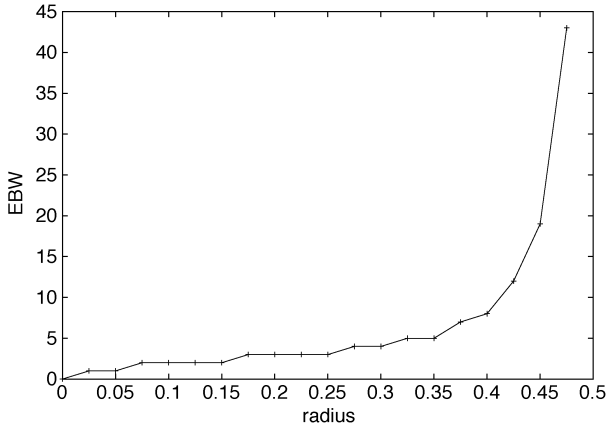

Fig. 4. EBW for a monopole of various radius (ρ') for cylinder with $a = 0.5\lambda$; EBW for incident field is $N = 5$.

the incident field EBW. Clearly, the coefficients converge to 0 quickly once $n > 5$.

2) MAS Monopole Case: Consider a single monopole inside the cylinder at some location (ρ', ϕ') labeled S in Fig. 1. The field strength is normalized to unit strength, i.e., $E_o = 1$. The electric field due to the monopole can be written

$$E_z^M = H_o^{(2)}\left(k|\vec{\rho} - \vec{\rho}'|\right) \tag{14}$$

where the superscript M indicates MAS monopole. Applying an addition theorem and computing the bandlimited form of E_z^M around a cylinder of radius a, we obtain

$$E_{z,N}^M = \frac{1}{2\pi}\sum_{n=-\infty}^{\infty} J_n(k\rho')H_n^{(2)}(ka)e^{-jn\phi'} \times \int_{\xi=0}^{2\pi} B_N(\phi,\xi)e^{jn\xi}d\xi \tag{15}$$

where an infinite absolute bandwidth is noted, as before.

Consider the location of the monopole. A monopole located at the origin has a constant field along the circular boundary. The EBW for a monopole at the origin is $N = 0$, which is easily verified using (3). However, as the monopole moves away from the origin, the EBW of the resultant field along the cylinder boundary increases.

Fig. 4 shows the numerically computed EBW for a monopole as it is moved from the origin toward the boundary of a cylinder with $a = 0.5\lambda$. Fig. 4 verifies the variation of the field due to a MAS monopole as the AS radius varies, as described in Section I. The variation (or EBW) of the incident field can now be compared to the EBW of the MAS monopole.

Assuming the incident field is a plane wave, the EBW for the incident field is $N = 5$. The monopole EBW matches the plane wave EBW at $\rho' = 0.325\lambda$. Certainly, choosing $\rho' > 0.325\lambda$ should result in solutions that are well-behaved in some sense, while choosing ρ' significantly less than 0.325λ may result in poorly behaved solutions. In other words, to avoid poor numerical accuracy, as described in [10], the AS radius should be chosen with a radius equal to or larger than $\rho' = 0.325\lambda$ for a cylinder of radius $a = 0.5\lambda$. Note that the AS radius depends on the incident field as well as the geometry of the scatterer.

III. Results and Discussion

In this section, example simulations based on the results of the previous section are discussed. A measure is introduced that quantifies whether the solution is stable (or well-behaved). The examples shall demonstrate the significance of the preceding development and the usefulness of EBW. In each case, the incident field is normalized to unit strength, i.e., $E_o = 1$.

The MAS formulation for the scattered field is a set of M_o monopoles at origins (ρ_m', ϕ_m')

$$E_z^s = \sum_{m=1}^{M_o} a_m H_o^{(2)}\left(k\left|\vec{\rho} - \vec{\rho}_m'\right|\right) \tag{16}$$

where $\vec{\rho}_m'$ is the vector from the origin to monopole m, and the coefficient a_m is the complex amplitude (or strength) of the m^{th} monopole. An example monopole location is shown in Fig. 1, labeled S. Generally, the monopoles are placed on an auxiliary surface (AS); for the cylinder, the AS is a circle with radius ρ'. The monopoles are equally spaced in ϕ around the AS, beginning with $\phi_1 = 0$.

The MAS method as implemented here computes the coefficients a_m using the system of linear equations

$$-E_z^i(\vec{\rho}_\ell) = \sum_{m=1}^{M_o} a_m H_o^{(2)}\left(k\left|\vec{\rho}_\ell - \vec{\rho}_m'\right|\right) \tag{17}$$

where $\vec{\rho}_\ell$ is a vector from the origin to the cylinder boundary at angle $\phi_\ell = 2(\ell-1)\pi/M_o$ and $\ell = 1, 2, \ldots, M_o$. The a_m are computed using an LU decomposition on the MAS matrix.

Typically, $\bar{\varepsilon}\%$, the average boundary condition error, is used to quantify the accuracy of the MAS solution. The average boundary condition error is computed using 360 points equally spaced along the boundary:

$$\bar{\varepsilon}\% = \frac{1}{360}\sum_{\phi=1}^{360^\circ}\frac{\left|E_z^i(\phi) + E_z^s(\phi)\right|}{\left|E_z^i(\phi)\right|} \times 100\%. \tag{18}$$

Before the simulation results are presented, the bandlimited form for the MAS scattered field (16) is computed. To compute the bandlimited form of the MAS series, (16) is substituted into (3), an addition theorem is applied and terms are rearranged to obtain

$$E_{z,N}^s = \frac{1}{2\pi}\sum_{n=-\infty}^{\infty} H_n^{(2)}(ka)\left[\sum_{m=1}^{M_o} a_m J_m\left(k\rho_m'\right)e^{-jn\phi_m'}\right] \times \int_{\xi=0}^{2\pi} B_N(\phi,\xi)e^{jn\xi}\,d\xi. \tag{19}$$

Comparing (19) to (13), it is apparent that the terms in brackets for each equation should be nearly equivalent for an accurate solution. Thus, if ρ_m' is small, then the $J_m(k\rho_m')$ terms may be much smaller than c_n in (13). The MAS solution will result

in $|a_m|$ that are very large. Next, consider (16) with very large $|a_m|$. To satisfy the boundary conditions, the coefficient phases will differ by nearly 180° to keep the magnitude of the scattered field on the order of the incident field. Coefficients a_m with large magnitude and oscillating phase are typically not stable and therefore not desirable.

Formally, the stability of numerical solutions can be inferred from the condition number of the matrix. The condition number can be estimated from the eigenvalues of the system as done for MAS in [10].

An alternative measure of stability is proposed here based on the a_m values of a particular solution. As described above, it is expected that poor stability will be characterized by large $|a_m|$ with phases differing by nearly 180°. To quantify this possible behavior of the coefficients, define a measure V as

$$V = \frac{|a_m|_{max}}{\frac{1}{M_o}\sum_{m=1}^{M_o} a_m} \tag{20}$$

where the numerator is the magnitude of the coefficient with the maximum magnitude; the denominator consists of an average of the coefficients and not the average of their magnitudes. Thus, large oscillating a_m will have a large numerator and a relatively small denominator in (20).

A. Monopole Line Source Incident Field

The performance of MAS for the circular cylinder in the presence of a monopole line source has been discussed in [8] and [9]. The monopole radius must enclose the singularities of the scattered field. For the circular cross section, the singularities are known to be at a radius of $\rho_{sing} = a^2/\rho''$ when the line source is at a radius ρ'', as shown in Fig. 1.

Calculation of the EBW for the monopole line source has been performed. It has been found that the MAS monopole radius required for the EBW of the scattered field closely matches the radius given by ρ_{sing}.

For example, with $a = 0.5\lambda$ and $\rho'' = 0.7\lambda$, EBW for the line source incident field is 6. The minimum MAS monopole radius using EBW is 0.375λ compared to $\rho_{sing} = 0.357\lambda$. Again for $a = 0.5\lambda$, placing the line source at $\rho'' = 0.6\lambda$, EBW calculations indicate an AS radius of 0.425λ, compared to $\rho_{sing} = 0.417\lambda$.

Consider a larger cylinder with radius $a = 1.25\lambda$. We shall now compare the EBW for a MAS monopole at AS radius $\rho' < 1.25\lambda$ and the EBW for a monopole line source at the corresponding ρ_{sing}, i.e., the line source is at $\rho'' = a^2/\rho'$.

Fig. 5 shows the comparison of EBW for the MAS pole and line source at the singular positions. The line source EBW becomes flat at $\mathrm{EBW} = 10$ since the line source has moved far enough away to approximate a plane wave source (approximately when $\rho' = 1\lambda$ or $\rho'' = 1.565\lambda$).

For q$\rho' > 1\lambda$, the EBW of the incident field matches closely the EBW of the MAS monopole. This verifies the result found previously; the poles should be on an AS of radius at least ρ_{sing}.

For $\rho' < 1\lambda$, the line source has $\mathrm{EBW} = 10$. This result matches the plane wave EBW for a cylinder with $a = 1.25\lambda$. Therefore, the AS radius must be larger than ρ_{sing} in this case. Certainly, there must be a minimum AS radius defined by the plane wave EBW. In the next section, we discuss this minimum AS radius.

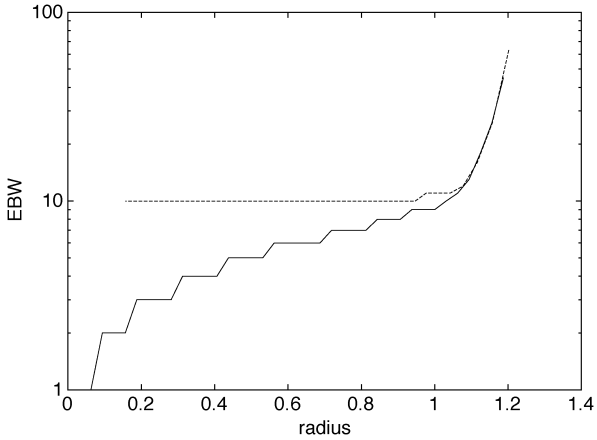

Fig. 5. Plot of EBW vs. MAS monopole radius for a 1.25λ radius cylinder. Solid line: the MAS monopole EBW ($\mathrm{radius} = \rho'$ in figure); dashed line: EBW for a line source at ρ'' corresponding to ρ_{sing} ($\mathrm{radius} = a^2/\rho''$ in figure).

TABLE I
MAS RESULTS ($a = 0.5\lambda$, PLANE WAVE INCIDENT FIELD)

ρ'_m	M_o	$\bar{\varepsilon}\%$	V
0.1	10	2.78	1,302
0.1	20	0.00106	23,846
0.3	10	5.48	7.93
0.3	20	0.0206	14.61
0.35	10	7.01	2.56
0.35	20	0.0892	3.50
0.4	10	12.14	1.63
0.4	20	0.644	1.51

B. Plane Wave Incident Field

A plane wave incident field can be considered as a special case of the monopole line source incident field where $\rho'' \to \infty$. For this limiting case, the singularity approaches the origin. In principle, the AS radius can be made very small. In [10], it is shown that a small AS radius can result in large numerical errors. In this section, it is shown that a minimum AS radius can be estimated using EBW results.

Consider a 0.5λ radius cylinder with a plane wave incident field as shown in Fig. 1. The EBW for the incident field is 5. The MAS results for $M_o = 10$ and 20 monopoles equally spaced in ϕ are summarized in Table I. The monopole radius is varied between $\rho'_m = 0.1$ and $\rho'_m = 0.4$.

For $\rho'_m = 0.1\lambda$, the EBW for the monopoles is 2 (recall, incident field EBW is 5). Table I shows the boundary condition error is less than 3% for 10 monopoles, and improves greatly for 20 monopoles. However, V is an excessively large number. The maximum coefficient magnitude (the numerator of V, $|a_m|_{max}$) is over 150 for 10 monopoles and is over 1,000 for 20 monopoles.

Choosing $\rho'_m = 0.3\lambda$, the monopole EBW is 3, a value closer to the incident field EBW of 5. Again, $\bar{\varepsilon}\%$ is small for $M_o = 10$ and improves greatly for $M_o = 20$. The measure V for 10 monopoles is much smaller than the $\rho'_m = 0.1\lambda$ case and nearly doubles for $M_o = 20$. Values of $|a_m|_{max}$ for $M_o = 10$, 20 are 1.91, 1.43, respectively. The solution for $\rho'_m = 0.3\lambda$ would be considered more stable than the $\rho'_m = 0.1\lambda$ solution.

For $\rho'_m = 0.35\lambda$, monopole EBW matches the incident field EBW of 5. The boundary condition error improves as M_o increases. The measure V is less than 4 and increases somewhat as M_o increases. Values of $|a_m|_{max}$ for $M_o = 10$ and 20 are 1.60 and 0.977, respectively.

Results for $\rho'_m = 0.4\lambda$ demonstrate that numerical accuracy has been achieved; the analytical accuracy now dominates the boundary condition error. To improve the solution accuracy, more monopoles are necessary. The stability of the solution, as indicated by smaller V, is expected to remain as M_o increases.

Simulations have been performed to investigate the effect of increasing M_o on V and $\bar{\varepsilon}\%$ for the case of $\rho_m = 0.4\lambda$ with $a = 0.5\lambda$. As M_o increases up to 50, V remains at approximately 1.5 while the average boundary condition error decreases.

In summary, it has been demonstrated that EBW can be used to obtain well-behaved solutions. In particular, the EBW of the MAS monopoles along the boundary must be equal to or greater than the EBW for the incident field to avoid numerical inaccuracies.

Optimization of a simulation by minimizing the boundary condition error may not guarantee suitable solutions. In Table I it can be seen that increasing MAS monopole radius for a fixed M_o increases $\bar{\varepsilon}\%$. However, the decreasing V as ρ'_m increases can be interpreted as obtaining solutions that are increasingly well-behaved. Certainly, when the scatterer is a more complex object, well-behaved solutions will be desired.

IV. Conclusions

In this work, the effective spatial bandwidth (EBW) of fields along the scatterer boundary has been introduced. The EBW for a variety of incident fields and scattered field models have been investigated. The EBW concept clearly indicates a lower limit for the radius of the MAS monopoles in both the plane wave incident field and the line source incident field cases. For the line source incident field, minimum AS radius as determined from EBW closely matches the well-known singularity radius. In general, the EBW of the MAS monopoles along the boundary must be equal to or greater than the EBW for the incident field to avoid numerical inaccuracies.

A measure, V, has been proposed and used to quantify the suitability of an MAS solution. It has been demonstrated that in some cases, the monopole coefficients have very large magnitudes and oscillating phases. The measure V is designed to extract the severity of this effect, and thus indicate whether a solution is well-behaved or not well-behaved.

The results reported here are for scatterers with a circular cross section; the concepts and tools developed can also be applied to scatterers with non-circular cross sections. However, for non-circular cross sections, application of the addition theorem will not result in the spatial harmonic content of the fields along the boundary; therefore, numerical methods to determine the EBW will be required.

References

[1] *Generalized Multipole Techniques for Electromagnetic and Light Scattering*, ser. Computational Methods in Mechanics, T. Wriedt, Ed.. New York: Elsevier Science, 1999, vol. 4.

[2] D. I. Kaklamani and H. T. Anastassiu, "Aspects of the method of auxiliary sources (MAS) in computational electromagnetics," *IEEE Antennas Propag. Mag.*, vol. 44, no. 3, pp. 48–64, Jun. 2002.

[3] F. Shubitidze, K. O'Neill, S. A. Haider, K. Sun, and K. D. Paulsen, "Application of the method of auxiliary sources to the wide-band electromagnetic induction problem," *IEEE Trans. Geosci. Remote Sens.*, vol. 40, no. 4, pp. 928–942, Apr. 2002.

[4] K. Beshir and J. Richie, "On the location and number of expansion centers for the generalized multipole technique," *IEEE Trans. Electromagn. Compat.*, vol. 38, no. 2, pp. 177–180, May 1996.

[5] E. Moreno, D. Erni, C. Hafner, and R. Vahldieck, "Multiple multipole method with automatic multipole setting applied to the simulation of surface plasmons in metallic nanostructures," *J. Opt. Soc. Amer. A*, vol. 19, no. 1, pp. 101–111, Jan. 2002.

[6] C. Hafner, *The Generalized Multipole Technique for Computational Electromagnetics*. Boston, MA: Artech House, 1990.

[7] P. B. Leuchtmann, "Automatic computation of optimum origins of the poles in the multiple multipole method (MMP method)," *IEEE Trans. Magn.*, vol. M-19, no. 6, pp. 2371–2374, Nov. 1983.

[8] Y. Leviatan, "Analytic continuation considerations when using generalized formulations for scattering problems," *IEEE Trans. Antennas Propag.*, vol. 38, no. 8, pp. 1259–1263, Aug. 1990.

[9] G. Fikioris, "On two types of convergence in the method of auxiliary sources," *IEEE Trans. Antennas Propag.*, vol. 54, no. 7, pp. 2022–2033, Jul. 2006.

[10] H. T. Anastassiu, D. G. Lymperopoulos, and D. I. Kaklamani, "Accuracy analysis and optimization of the method of auxiliary sources (MAS) for scattering by a circular cylinder," *IEEE Trans. Antennas Propag.*, vol. 52, no. 6, pp. 1541–1547, Jun. 2004.

[11] M. Abramowitz and I. A. Stegun, *Handbook of Mathematical Functions*. New York: Dover, 1965.

[12] O. M. Bucci and G. Franceschetti, "On the spatial bandwidth of scattered fields," *IEEE Trans. Antennas Propag.*, vol. 35, no. 12, pp. 1445–1455, Dec. 1987.

James E. Richie (M'80–SM'96) received the B.S. degree in electrical engineering from Lafayette College, Easton, PA, in 1983, and the M.S. (electrical engineering) and Ph.D. degrees from the University of Pennsylvania, Philadelphia, in 1985 and 1988, respectively.

He has been on the faculty of the Electrical and Computer Engineering Department, Marquette University, Milwaukee, WI, since 1988, where he is currently an Associate Professor and Coordinator of the Electrical Engineering Program.

Dr. Richie is a member of Tau Beta Pi, Eta Kappa Nu, and Sigma Xi.